

## **A disulfur-ligand stabilization approach to construct silver(I)-cluster-based porous framework as highly sensitive SERS substrate**

Tong Wu,<sup>a, †</sup> Di Yin,<sup>a †</sup> Xun Hu,<sup>a</sup> Bo Yang,<sup>b</sup> Hong Liu,<sup>\*a, d</sup> Yun-Peng Xie,<sup>c</sup> Shi-Xi Liu,<sup>\*b</sup> Lulu Ma,<sup>a</sup> and Guang-Gang Gao<sup>\*a, d</sup>

<sup>a</sup> School of Materials Science and Engineering, University of Jinan, Jinan, 250022, China.

<sup>b</sup> School of Chemical Science and Technology, Yunnan University, Kunming 650091, China

<sup>c</sup> School of Materials Science and Engineering, Huazhong University of Science and Technology, Wuhan 430074, China

<sup>d</sup> College of Pharmacy, Jiamusi University, Jiamusi 154007, China.

E-mail: mse\_liuh@ujn.edu.cn; shxliu@ynu.edu.cn; mse\_gaogg@ujn.edu.cn

## Materials and Characterization

**Materials.** All chemicals and solvents obtained from the supplier are used without further purification. All solvents are analytical grade reagents.

### Characterization Instrumentation.

TG curves were performed on a Perkin-Elmer TGA analyzer heated from room temperature to 1000 °C under nitrogen gas with a heating rate of 10 °C/min. Elemental analyses for C N and H were performed on a Perkin-Elmer 240C analyzer. Powder Xray diffraction (PXRD) data for **Ag<sub>11</sub>**, **UJN-1** and their reduction samples were collected on a Rigaku D/Max-2500PC diffractometer with Cu K $\alpha$  radiation ( $\lambda = 1.5418 \text{ \AA}$ ) over the  $2\theta$  range of 10-20° at room temperature. In order to investigate the stoichiometry of states for Ag atoms, the software XPSPEAK 4.1 was applied to fit the data. FTIR spectra were recorded in the 500-4000  $\text{cm}^{-1}$  region on an Alpha Centaur FT/IR spectrophotometer (KBr pellets). TEM images were measured on a JEM-2100 transmission electron microscope operated at an acceleration voltage of 200 kV. In the preparation of **UJN-1** and the reduced **UJN-1** for TEM observation, the samples were firstly dispersed in methanol using an ultrasonic bath and then dropped onto copper grid, which was dried in air at room temperature and kept in vacuum for 20 min before TEM observation. During the TEM detection, after the electron beam irradiates to the samples, the observing time can not exceed more than 30 min to avoid the reduction of the Ag(I) species in the samples. For **UJN-1** sample, we only observed the clear electron diffraction points of the higher order (332), (422), and (510) crystal facets. On the one hand, this is due to that these facets correspond to the higher  $2\theta$  values of 11.3° , 11.8° and 12.3° , respectively. While the  $2\theta$  values for (211), (310) and (321) plane facets are 5.9° , 7.6° and 9.0° , respectively. During the detection of electron diffraction, the crystal sample should be in a suitable position to obtain the strong diffraction points, which is more difficult for the lower  $2\theta$  facets. On the other hand, no strong diffraction peaks can be observed in the XRD patterns within the small  $2\theta$  range, indicating that the nanosized samples of **UJN-1** may expose more higher order crystal facets of (332), (422), and (510) than the lower order ones. In the reduced **UJN-1** sample, the observed crystal facets of (422) and (510) also confirm the stability of high order facets. The software NANO MEASURER 1.2 was applied to calculate the particle size of nanoclusters.

## X-ray Crystallography.

Crystal data were collected on an Agilent Technology Eos Dual system with focusing multilayer mirror optics and a Mo K $\alpha$  source of  $\lambda = 0.71073 \text{ \AA}$ . Empirical absorption corrections were applied to the intensities using the SADABS program. The structures were solved using the program SHELXS97 and refined with the program SHELXL-97. The positions of the metal atoms and their first coordination spheres were located from direct-methods. Other non-hydrogen atoms were found in alternating difference Fourier syntheses and least-squares refinement cycles. During the final cycles, except for some C atoms or some solvent molecules, all other non-hydrogen atoms were refined anisotropically. Hydrogen atoms were placed in calculated positions refined using idealized geometries and assigned fixed isotropic displacement parameters.

## DFT calculation

DFT optimization was performed by Gaussian 09 program<sup>[1]</sup> at B3PW91 level. The LANL2DZ basis set was used for silver atoms and the 6-31G(d) basis set was employed for other atoms. Ag<sub>5</sub> subunit was keeping high symmetry, which point group was S<sub>4</sub>, during the optimization. In contrast, Ag<sub>9</sub> subunit and Ag<sub>11</sub> lost their symmetry after optimization. The HOMO, LUMO schematic diagrams were obtained by VESTA package<sup>[2]</sup> Version 3.4.3.

## Reference

[1] Gaussian 09, Revision E.01, M. J. Frisch, G. W. Trucks, H. B. Schlegel, G. E. Scuseria, M. A. Robb, J. R. Cheeseman, G. Scalmani, V. Barone, B. Mennucci, G. A. Petersson, H. Nakatsuji, M. Caricato, X. Li, H. P. Hratchian, A. F. Izmaylov, J. Bloino, G. Zheng, J. L. Sonnenberg, M. Hada, M. Ehara, K. Toyota, R. Fukuda, J. Hasegawa, M. Ishida, T. Nakajima, Y. Honda, O. Kitao, H. Nakai, T. Vreven, J. A. Montgomery, Jr., J. E. Peralta, F. Ogliaro, M. Bearpark, J. J. Heyd, E. Brothers, K. N. Kudin, V. N. Staroverov, T. Keith, R. Kobayashi, J. Normand, K. Raghavachari, A. Rendell, J. C. Burant, S. S. Iyengar, J. Tomasi, M. Cossi, N. Rega, J. M. Millam, M. Klene, J. E. Knox, J. B. Cross, V. Bakken, C. Adamo, J. Jaramillo, R. Gomperts, R. E. Stratmann, O. Yazyev, A. J. Austin, R. Cammi, C. Pomelli, J. W. Ochterski, R. L. Martin, K. Morokuma, V. G. Zakrzewski, G. A. Voth, P. Salvador, J. J. Dannenberg, S. Dapprich, A. D. Daniels, O. Farkas, J. B. Foresman, J. V. Ortiz, J. Cioslowski, and D. J. Fox, Gaussian, Inc., Wallingford CT, 2013.

[2] K. Momma, F. Izumi, *J. Appl. Crystallogr.*, 2011, **44**, 1272-1276.

## Supporting Figures

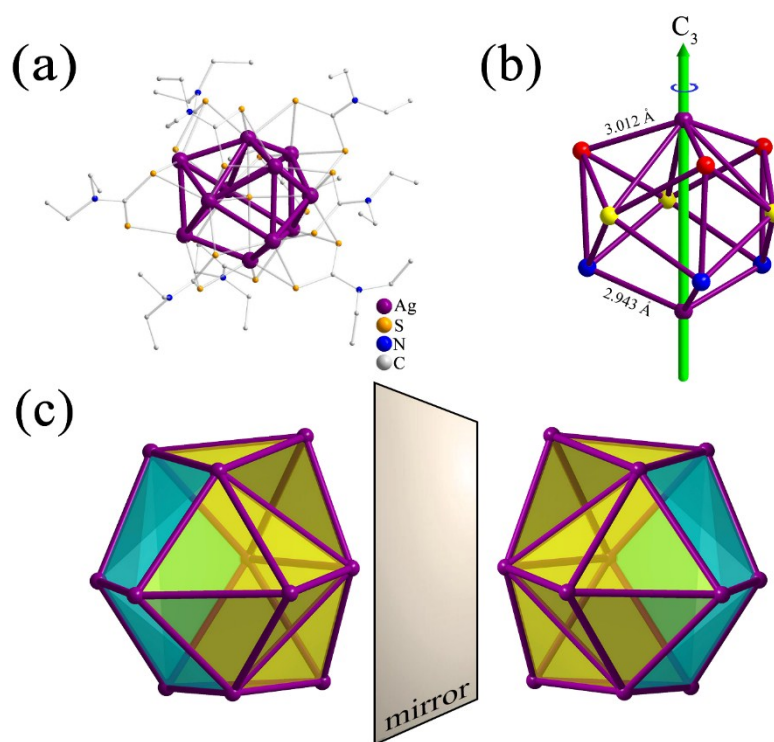


**Fig. S1** (a) Crystal structure of  $\text{Ag}_{11}$ ; (b) Structure of  $\text{Ag}\cdots\text{Ag}$  interactions induced 11-core silver(I) cluster; (c) Chirality representation of  $\text{Ag}_{11}$ .

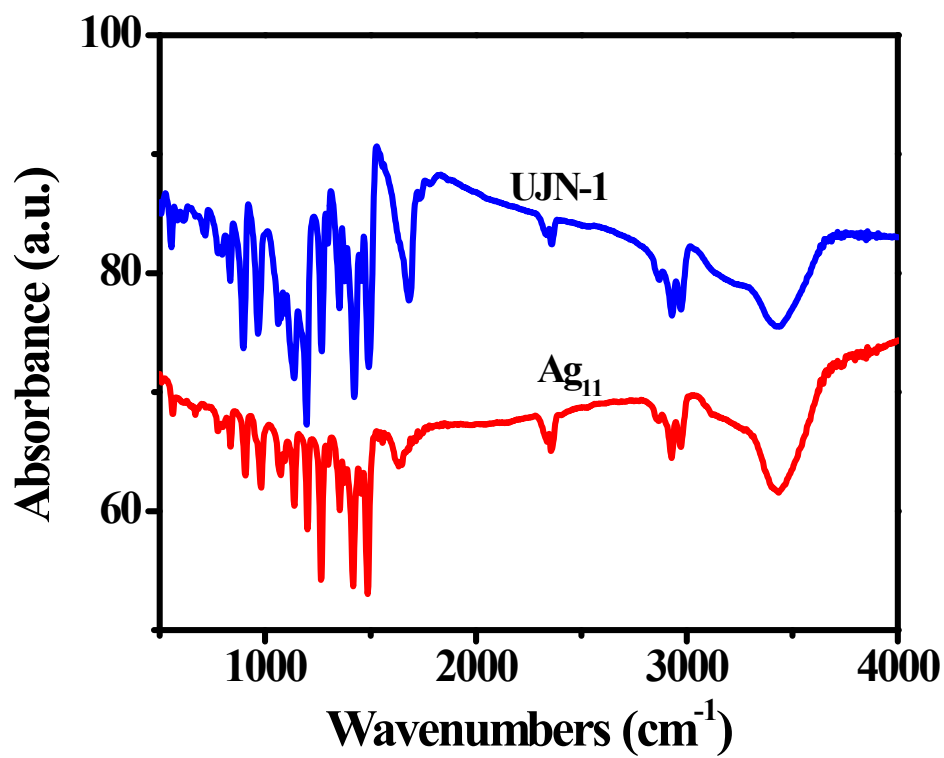


**Fig. S2** FTIR spectra of UJN-1 and Ag<sub>11</sub>.

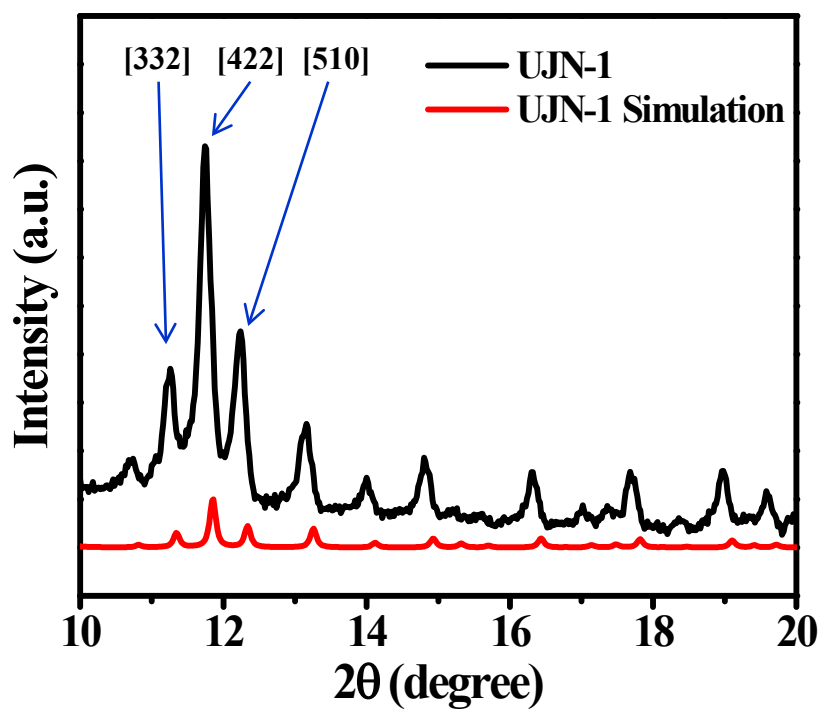


**Fig. S3** The XPRD patterns for UJN-1 (the red line is the simulated curve).

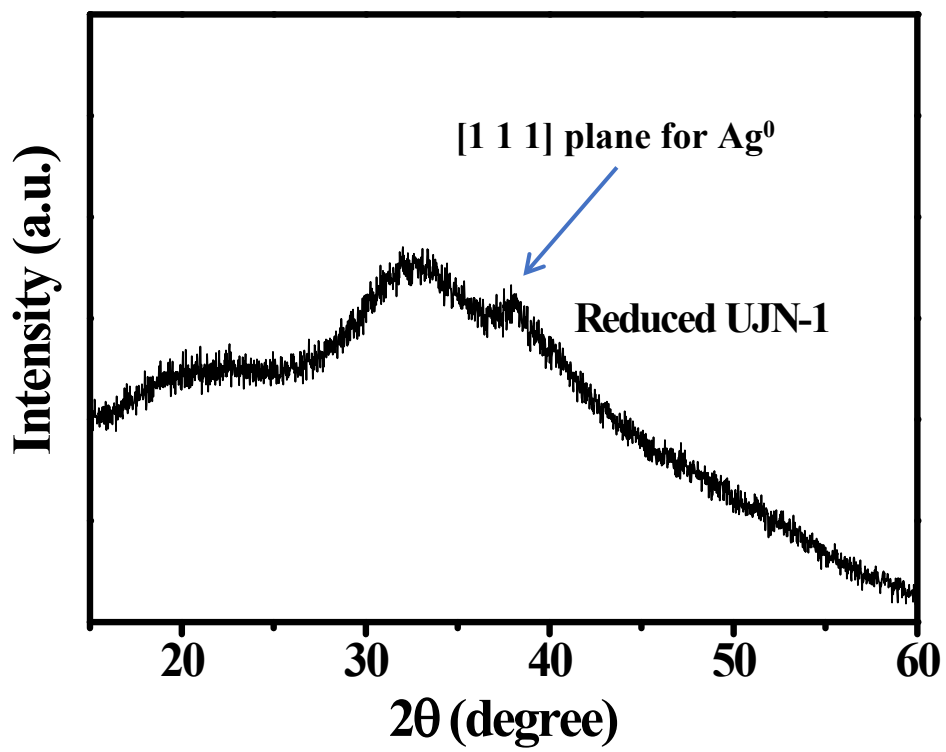


Fig. S4 The XPRD patterns for reduced UJN-1.

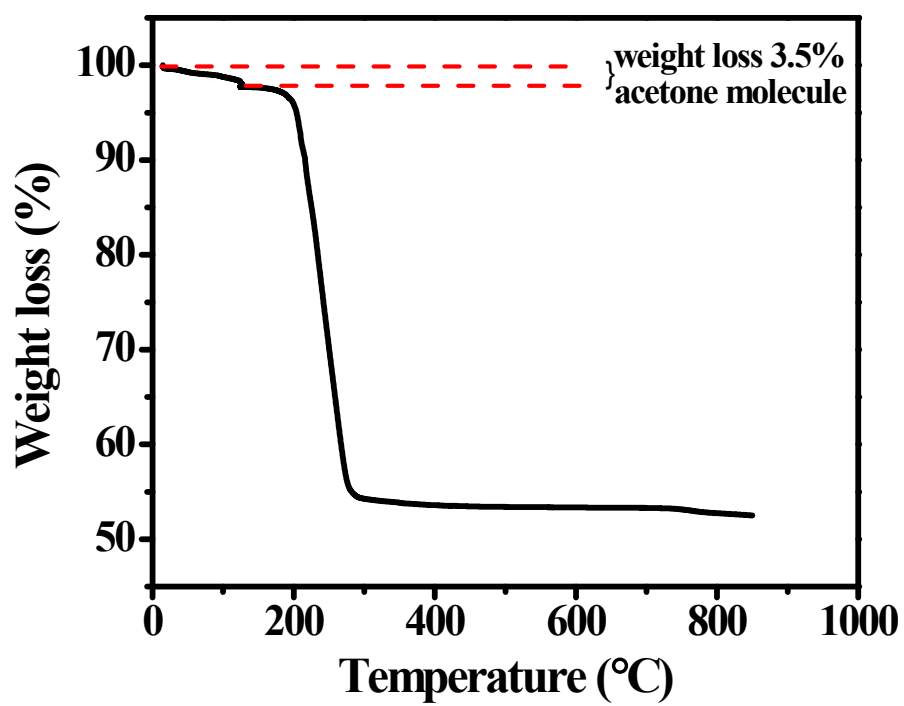


Fig. S5 TGA plot of UJN-1.



## Crystallographic data

### Crystallographic data for UJN-1 and Ag<sub>11</sub>

Compound	UJN-1	Ag <sub>11</sub>
Empirical formula	C <sub>210</sub> H <sub>420</sub> Ag <sub>51</sub> N <sub>42</sub> S <sub>84</sub>	C <sub>45</sub> H <sub>84</sub> Ag <sub>11</sub> N <sub>9</sub> S <sub>19</sub>
Formula weight	11728.28	2546.92
Temperature/K	293(2)	293(2)
Crystal system	Cubic	Cubic
Space group	I -4 3 d	I 2 3
<i>a</i> /Å	36.5504(7)	26.0410(3)
<i>b</i> /Å	36.5504(7)	26.0410(3)
<i>c</i> /Å	36.5504(7)	26.0410(3)
$\alpha$ /°	90	90
$\beta$ /°	90	90
$\gamma$ /°	90	90
Volume/Å <sup>3</sup>	48829.0(3)	17659.3(6)
<i>Z</i>	4	8
$\rho_{\text{calc}}$ /g/cm <sup>3</sup>	1.547	1.202
Absorption coefficient/mm <sup>-1</sup>	19.629	2.595
<i>F</i> (000)	21321	5779
$\lambda$ /Å	0.710	0.710
Limiting indices	-41 ≤ <i>h</i> ≤ 18, -42 ≤ <i>k</i> ≤ 36, -18 ≤ <i>l</i> ≤ 33	-31 ≤ <i>h</i> ≤ 26, -31 ≤ <i>k</i> ≤ 31, -26 ≤ <i>l</i> ≤ 31
Reflections collected	19440	63104
Independent reflections	6184	5387
<i>R</i> <sub>(int)</sub>	0.0274	0.0725
Data/restraints/parameters	6184/0/299	5387/0/250
Goodness-of-fit on <i>F</i> <sup>2</sup>	1.084	1.098
<i>R</i> <sub>1</sub> <sup><i>a</i></sup> , <i>wR</i> <sub>2</sub> <sup><i>b</i></sup> [ <i>I</i> > 2σ( <i>I</i> )]	0.0737, 0.2215	0.0525, 0.1452
<i>R</i> <sub>1</sub> <sup><i>a</i></sup> , <i>wR</i> <sub>2</sub> <sup><i>b</i></sup> [all data]	0.0937, 0.2430	0.0636, 0.1531

$$^a R_1 = \sum ||F_o| - |F_c|| / \sum |F_o|, \quad ^b wR_2 = \sqrt{\frac{\sum w(|F_o|^2 - |F_c|^2)^2}{\sum w(F_o^2)^2}}^{1/2}.$$